Indirect Detection of the Protons in and Around Biradicals and their Mechanistic Role in MAS-DNP

Satyaki Chatterjee,[a] Faith J. Scott,[b] Snorri Th. Sigurdsson,[a] Amrit Venkatesh,[b]

Frédéric Mentink-Vigier[b,c]*

a. *University of Iceland, Department of Chemistry, Science Institute, Dunhaga 3, 107 Reykjavik (Iceland)*

b. *National High Magnetic Field Laboratory, Florida State University, 1800 E. Paul Dirac Dr, Tallahassee, FL, 32310, USA*

c. *Department of Chemistry and Biochemistry, Florida State University, Tallahassee, FL 32306, USA.*

Corresponding Authors

fmentink@fsu.edu

ABSTRACT

The contribution of protons on or near biradical polarizing agents in Dynamic Nuclear Polarization (DNP) has recently been under scrutiny. Results from selective deuteration and simulations have previously suggested that the role of protons on the biradical molecule depends on the strength of the electron-electron coupling. Here we use the cross effect DNP mechanism to identify and acquire ^{1}H solid-state NMR spectra of the protons that contribute to propagation of the hyperpolarization, via an experimental approach dubbed Nuclear Double Resonance (NUDOR).

KEYWORDS Hyperpolarization, electron-electron interactions, Double Resonance, Cross-Effect, ENDOR

The weak coupling between nuclear spins and the magnetic field in Nuclear Magnetic Resonance (NMR) spectroscopy generates low nuclear spin polarization, which results in low signal-to-noise ratios and a long signal acquisition times.[1,2] Dynamic Nuclear Polarization (DNP) uses the strong coupling of unpaired electron spins with the magnetic field to increase the sensitivity of solid-state NMR, with numerous reported applications in material science and biology.[3–8] A combination of Magic Angle Spinning (MAS) and DNP has been shown to yield high resolution and sensitivity in solid-state NMR.[2–6]

The unpaired electrons, that are often provided by biradical polarizing agents,[2,9,10] are typically used to hyperpolarize protons (^{1}H) using the cross effect (CE) mechanism under MAS.[11–18] Briefly, in CE DNP, the nuclear spins that are close to the biradical are hyperpolarized due to the presence of electron-nuclear hyperfine interactions, and ^{1}H-^{1}H homonuclear spin diffusion equilibrates this hyperpolarization with protons that are further away.

The protons on the biradicals have strong hyperfine couplings to the electron spins, which contains both isotropic and anisotropic components on the order of several MHz (see Fig. S6). This coupling renders the spectra of such protons very broad and below the detection limit.[19,20] The hyperfine couplings modify the Larmor frequency and thus impacts the propagation of the spin hyperpolarization; this correlation is at the centre of the concept called "spin diffusion barrier".[19–22] The situation is similar to heteronuclear spin diffusion,[23–26] and the importance of this "spin diffusion barrier" for MAS DNP has been debated.[20,27,28] However, large spin system simulations have indicated that quantitative results can be obtained only if the protons on the biradical are considered,[25,26,29,30] and the importance of these protons has been shown experimentally via selective deuteration.[27,31,32] As the protons that are proximal to the unpaired

electron spin are critical to MAS DNP, it is of great interest to detect them via NMR, at least by indirect means.

In this Letter, we introduce a Nuclear-Nuclear Double Resonance (NUDOR) technique to indirectly detect protons in and around biradicals and analyze their role in the cross effect DNP mechanism. The approach, which uses off-resonance irradiation (**Fig. 1**), produces data analogous to an Electron-Nuclear Double Resonance (ENDOR)[33] experiment. This NUDOR experiment is used to show that in biradicals like TEKPol[34] and AMUPol,[35] the strongly coupled protons on the biradicals play an essential role in MAS DNP. It also proves that these strongly coupled protons are not critical for the performance of a biradical called AsymPol-TEK.[36] This was further validated by evaluating a series of partially deuterated derivatives, confirming that the protons on AsymPol-TEK biradicals do not significantly contribute to DNP because of strong electron-electron interactions within the molecule.[28] This insight is valuable for designing future biradicals, as it indicates that proton involvement may not be as critical in certain cases due to these electron interactions.

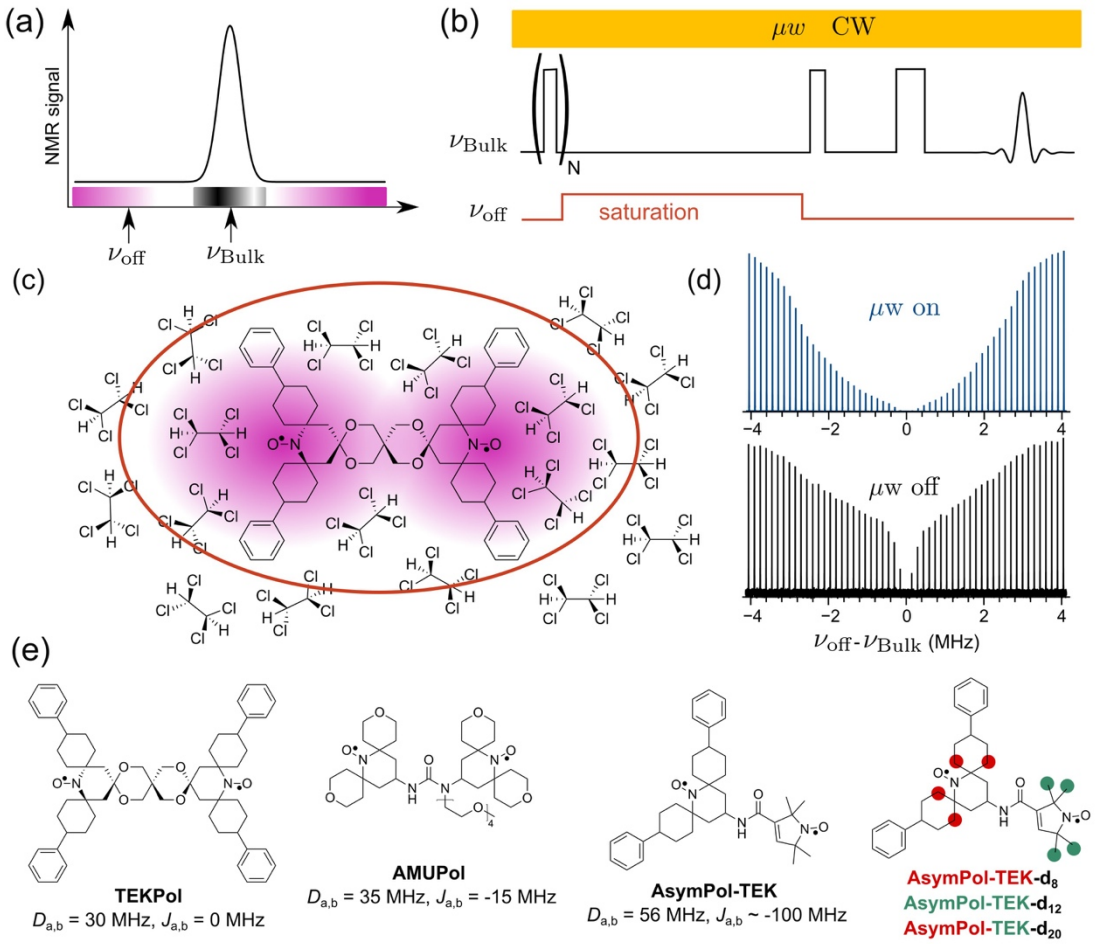

Fig. 1. (a) Schematic of a ^{1}H NMR spectrum and position of the on-resonance (ν_{Bulk}) and off-resonance (ν_{off}) radiofrequency (rf) irradiations. (b) Pulse sequence used for NUDOR: the bulk protons are first presaturated and subsequently a long off-resonance saturation pulse (~500 ms, 15 kHz rf) is applied, followed by detection of the bulk protons with an echo sequence. The resulting spectra are collected with and without μw irradiation. (c) Structure of the biradical TEKPol in a frozen 1,1,2,2-tetrachloroethane (TCE) solution. The purple color indicates the radius for hyperfine coupling; the gradient illustrates the strength of the coupling. The oval circle (red) represents the volume of the protons that are saturated by the ν_{off} irradiation. (d) Example of the NUDOR profile for TEKPol with and without μw irradiation. (e) Structures of the biradicals studied using NUDOR in this work.

Probing otherwise invisible spins, using observable NMR or EPR signals, is well-known in magnetic resonance.[37–39] In EPR, the ELDOR experiment relies on the irradiation of forbidden transitions to observe nuclei in close proximity to the electron spin. In NMR, the widely utilized Chemical Exchange Saturation Transfer (CEST)[37] relies on weak radiofrequency (rf) fields to saturate invisible protons, which affects the observable proton spins by chemical exchange. Similarly, one can use the homonuclear spin diffusion instead of the chemical exchange to detect a site of interest. This is used, for example, in Progressive Saturation of the Proton Reservoir (PROSPR).[40] Here, the pulse sequence is dubbed NUDOR in reference to the Electron-Electron Double Resonance (ELDOR).[41,42]

The idea behind the experiment described here is that if the unobservable, strongly-coupled protons (i.e. protons that are strongly hyperfine coupled to the electron spins) on or near the biradical molecules contribute to the DNP mechanism, the signal intensity (I) of the observable bulk proton spin bath, with and without microwave (μw) irradiation (denoted by the DNP enhancement factor, $\epsilon_{\mathrm{on/off}} = I_{\mathrm{on}}/I_{\mathrm{off}}$), can be modulated by perturbing the spin states of the strongly coupled nuclei. This hypothesis would be valid if the strongly-coupled protons are essential to the DNP mechanism (*vide infra*). The NMR spectrum of the biradical protons (purple region) span a much higher frequency range than the spectrum of the bulk protons (black region, **Fig. 1a**), due to the strong hyperfine couplings with the unpaired electrons. In NUDOR, the initial pulse train presaturates the bulk proton signal and subsequently, a long and low power saturation pulse (500 ms at a rf nutation of 15 kHz) is applied at a frequency ν_{off}, where ν_{off} is an off-resonance frequency with respect to the observable bulk proton signal. Finally, the signal of the bulk protons is detected using a spin echo sequence at the frequency ν_{Bulk} (**Fig. 1b**). Changing the offset corresponds to changing the radius of a shell surrounding each radical: the protons located

within this radius are partially saturated (**Fig. 1c**). Then, spin diffusion transports this saturation to the observable bulk signal. MAS modulates the electron-nuclear hyperfine couplings, which results in a spread of the saturation across a wider frequency range, and also results in more efficient spin diffusion due to nuclear dipolar rotor events.[10,24,43] The effect of the pulse sequence can be easily reproduced with standard spin dynamics simulations on a three-spin system (see Fig. S5).

A series of 1D ^{1}H solid-state NMR spectra can be obtained at ν_{Bulk} by varying ν_{off}. The experiments are performed in the presence and absence of μw irradiation to probe the involvement of the protons in the DNP mechanism. Taking the ratios of the μw on and off signal intensities also limits the distortion of the profile due to the rf properties of the NMR probe (see SI). An example of the effect of the variable off-resonance irradiation is shown in **Fig. 1d** for the biradical TEKPol (**Fig. 1e**), both in the presence and absence of μw irradiation. In both cases, the off-resonance irradiation impacts the bulk NMR signal intensity up to $|\nu_{\mathrm{off}} - \nu_{\mathrm{Bulk}}| \approx 4$ MHz. The proposed NUDOR experiment is also analogous to the SPIDEST experiment[44] but uses continuous-wave irradiation combined with the DNP enhancement factors to obtain the "hyperfine-shifted" spectra.[44]

Fig. 2a shows the NUDOR profile, i.e. the normalized DNP enhancement factor plotted as a function of ν_{off}, for AMUPol in glycerol-d_8/D_2O/H_2O (6/4/1 vol %) and TEKPol in 1,1,2,2-tetrachloroethane (denoted as TCE). The profiles are normalized with respect to the reference DNP enhancement factor obtained in the absence of the saturation pulse. As expected, the enhancement is null when $\nu_{\mathrm{off}} = \nu_{\mathrm{Bulk}}$ since the on-resonance saturation nullifies the bulk signal. As the irradiation frequency of the saturation pulse is shifted away from the bulk resonance, the

enhancement increases. Once the off-resonance saturation pulse is applied beyond 4 MHz, the observed NUDOR enhancement is equal to the reference DNP enhancement factor, i.e. when obtained without the saturation pulse. Interestingly, the NUDOR profiles show features that can be compared to the theoretical ENDOR spectra (**Fig. 2a**, dashed lines). The calculated ENDOR spectra were obtained with EasySpin[45,46] using the hyperfine couplings calculated via DFT (see SI). The total widths of the experimental NUDOR profiles and calculated ENDOR spectra correlate well and features of the ENDOR spectra can be observed in the NUDOR experiment (**Fig. 2a**). For example, the shoulders near +2 and –2 MHz in the NUDOR profiles of both TEKPol and AMUPol are reproduced in the calculated ENDOR spectra. Note that a better match between NUDOR and ENDOR for AMUPol can be obtained by using lower power saturation pulses (10 kHz rf, see **Fig. S3a**) – this comparison confirms that the NUDOR experiment indeed senses the nuclei in the vicinity of the biradical.

For AMUPol and TEKPol, the NUDOR experiments show that 50% of the enhancement is recovered at $|\nu_{\mathrm{off}}^{50\%} - \nu_{\mathrm{Bulk}}| \approx 2$ MHz; such large 2 MHz hyperfine couplings correspond to protons located proximate to the nitroxide (NO•) group (located within ca. 0.35 nm; the corresponding spheres are shown in **Fig. 2c**). Since TEKPol and AMUPol have modest electron-electron couplings,[47] they may be inefficient at *directly* hyperpolarizing the bulk medium.[16,27,28] Indeed, the rate at which the CE polarizes the nuclei (R_{CE}) can be approximated as:

$$R_{\mathrm{CE}} \propto \left(\frac{\langle (D_{a,b} + 2J_{a,b})^2 \rangle \langle \left(A_{a,n}^{\pm} - A_{b,n}^{\pm} \right)^2 \rangle}{\omega_n^2} \right) \qquad (1)$$

where $D_{a,b}$ and $J_{a,b}$ are the electron-electron dipolar coupling and the exchange interaction, respectively. $A_{a,n}^{\pm}$ and $A_{b,n}^{\pm}$ are the pseudo-secular hyperfine coupling to the nucleus n and ω_n is

the nuclear Larmor frequency.[16,28] This relation shows that for a moderate $\langle (D_{a,b} + 2J_{a,b})^2 \rangle$, stronger $\langle \left(A^{\pm}_{a,n} - A^{\pm}_{b,n}\right)^2 \rangle$ is required for efficient polarization. The NUDOR experiments thus confirm that the protons on the biradicals AMUPol and TEKPol are critical for the hyperpolarization transfer. This result is entirely consistent with the previous experimental observations with TEKPol.[27]

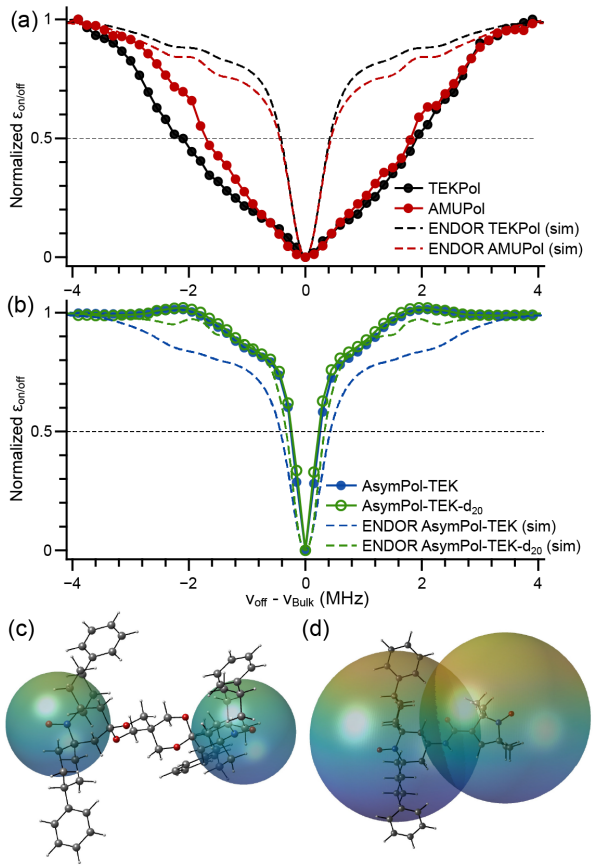

Fig. 2. NUDOR profiles of (a) 16 mM TEKPol in TCE (black) and 10 mM AMUPol in glycerol-d_8/D_2O/H_2O (6/4/1 vol %) (red), and (b) 10 mM AsymPol-TEK (blue) and 10 mM AsymPol-TEK-d_{20} (green) in TCE. Dashed lines correspond to simulated ENDOR spectra. (c) Sphere of 0.35 nm around the NO• group of TEKPol, corresponding to $|\nu_{\mathrm{off}}^{50\%} - \nu_{\mathrm{Bulk}}| \approx 2$ MHz. (d) Sphere of 0.7 nm around the NO• group of AsymPol-TEK corresponding to $|\nu_{\mathrm{off}}^{50\%} - \nu_{\mathrm{Bulk}}| \approx 0.2$ MHz.

On the other hand, we have previously used deuterated AsymPol biradicals and extensive large spin-system simulations to show that the protons on the AsymPol biradicals play a limited role in polarization transfer.[16,28] To experimentally confirm this notion, the NUDOR experiment was applied to two biradicals in the AsymPol family: AsymPol-TEK[36] and AsymPol-TEK-d_{20}, which has been newly synthesized and reported here (**Fig. 1d**). These radicals are identical, except that the protons with the largest hyperfine couplings have been replaced with deuterons in AsymPol-TEK-d_{20} (for synthesis, see SI). The results are striking: the NUDOR profiles of both biradicals are identical, showing that the protons that were replaced by deuterons do not participate in the DNP mechanism (**Fig. 2b**). In both cases, a narrow component close to the bulk resonance frequency is observed, and at further off-resonance frequencies, the enhancement recovers sharply back to the reference value. The NUDOR profiles of AsymPol-TEK and AsymPol-TEK-d_{20} are identical, which is different from the expected ENDOR spectra. Indeed, according to the ENDOR simulations, the two biradicals should have strikingly different NUDOR profiles (dotted lines **Fig. 2b**). In particular, the predicted ENDOR spectrum of AsymPol-TEK shows signals in the region ranging from 1.5-3 MHz. However, these features are not observed in the experimental NUDOR profiles, which demonstrates that saturating or removing a few of the most strongly coupled nuclear spins in AsymPol-TEK (i.e. the protons closest to the nitroxide moieties), does not affect the CE DNP process. This means that the first protons being hyperpolarized must be located outside the biradical molecule, i.e. the solvent, similar to our previous observation with AsymPol derivatives.[28]

An intriguing observation for AsymPol-TEK is that at $\left|\nu_{\mathrm{off}} - \nu_{\mathrm{Bulk}}\right| \approx 2$ MHz, there is a reproducible overshoot of the enhancement by ~ 1-2 %. Note that the actual signal intensity did

not increase with respect to the reference experiment without saturation (see **Fig. S2**). Rationalizing this minor observation is beyond the scope of this work.

In the case of AsymPol-TEK, 50% of the enhancement is recovered at $|\nu_{\mathrm{off}}^{50\%} - \nu_{\mathrm{Bulk}}| \approx 0.2$ MHz, corresponding to a factor ~10 smaller than with AMUPol or TEKPol. This value agrees with the ratio of electron-electron spin couplings:[25,28,48]

$$\frac{\langle (D_{a,b} + 2J_{a,b})^2 \rangle_{\mathrm{AsymPol-TEK}}}{\langle (D_{a,b} + 2J_{a,b})^2 \rangle_{\mathrm{TEKPol}}} \sim 30 \tag{2}$$

$$\frac{\langle (D_{a,b} + 2J_{a,b})^2 \rangle_{\mathrm{AsymPol-TEK}}}{\langle (D_{a,b} + 2J_{a,b})^2 \rangle_{\mathrm{AMUPol}}} \sim 10 \tag{3}$$

A hyperfine coupling value of 0.2 MHz corresponds to protons located at ~0.7 nm, i.e., relatively far from the NO$^{\bullet}$ as depicted in **Fig. 2d**. Thus, for AsymPol-TEK, only protons that are not in the vicinity of the nitroxide (i.e. those that are either far on the backbone or in the solvent), are essential for DNP. To further confirm this observation, selectively deuterated derivatives AsymPol-TEK-d_8 and AsymPol-TEK-d_{12} were synthesized (see SI), in addition to the aforementioned AsymPol-TEK-d_{20} (**Fig. 1e**), in which the protons with the strongest hyperfine couplings are removed. The DNP enhancement and characteristic DNP buildup time (T_B) for these compounds are shown in **Fig. 3a** and **3b**, respectively. The enhancements are similar for all isotopologues and fall in the range between 50 and 58. Some variation is observed in the buildup times, ranging from 1.6 to 2.3 s. The fact that the enhancements are similar, supports the idea that the strongly coupled protons do not play an essential role in the DNP. This is in stark contrast to TEKPol, where smaller enhancements were obtained upon deuteration.[27,28] It should be noted that the variations in the build-up times, which may appear at first to follow the previous trends observed by Venkatesh *et*

al. of increased build-up times with more deuteration,[27] was found to be due to slightly lower concentrations of the deuterated samples.

The AsymPol-TEKs should have the same geometry/magnetic parameters as previously reported,[36] because their liquid state EPR spectra are identical (**Fig. S4**). Accounting for the differences in concentration of the biradicals, it is possible to perform quantitative quantum simulations. Using large spin system simulations[24,25,29] and DFT/Molecular Dynamics[25,29] as input parameters for the hyperfine couplings on the biradicals, both the enhancements and buildup time are very well reproduced (**Fig. 3**). As the MAS-DNP simulations are quantitatively accurate, we used them to check the impact of deuteration, assuming identical biradical concentration. The results (**Fig. S7**) indicate that identical buildup should indeed be expected for all deuteration levels. As such, this confirms the outcome of previous work[16,28] and of the NUDOR experiments: AsymPol-TEK predominantly hyperpolarizes the protons of the solvent directly, and that the relayed hyperpolarization through the protons on the biradicals is less favorable.

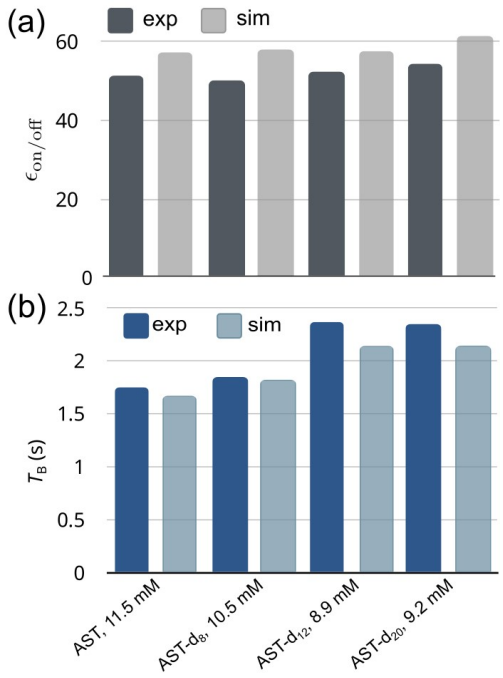

Fig. 3. Evolution of (a) DNP enhancements and (b) build-up time as a function of deuteration level in AsymPol-TEK. In (a), experiments and simulations are shown in dark and light grey, respectively, and in (b) experiments and simulations are shown in dark and light blue, respectively.

In summary, we have shown that NUDOR can be used to detect strongly coupled protons on nitroxide biradicals. This experiment allows identification of the protons that are essential for the DNP process. At 14.1 T, it provides a definite and direct proof that the protons on the biradicals of TEKPol and AMUPol contribute to the DNP under MAS, while the protons on the AsymPols play a minor role in the DNP process, as previously proposed.[28] We anticipate that the NUDOR profiles for a given biradical may depend on the experimental conditions, such as the magnetic field and the MAS frequency, as well as the length and rf power of the saturation pulse. It is likely that the $\nu_{\mathrm{off}}^{50\%}$ of AsymPol-TEK will increase at higher field as R_{CE} diminishes, meaning that protons on the biradical may play a greater role at higher fields. Reciprocally, the $\nu_{\mathrm{off}}^{50\%}$ should

decrease for AMUPol and TEKPol as the field is lowered. The NUDOR experiment thus provides a simple way to tune the properties of a given biradical for a set of experimental conditions. Finally, it may be possible to apply the method to other polarizing agents, such as monoradicals[49,50] or metal ions[51], to determine, at least partially, the ENDOR spectra of nuclear spins that are very close to the electron, without the need of an EPR instrument.

ASSOCIATED CONTENT

Experimental details and derivation of the equations are available in the Supporting Information

The following files are available free of charge.

Supporting information:

AUTHOR INFORMATION

Corresponding Author

Frédéric Mentink-Vigier: National High Magnetic Field Laboratory, Florida State University, 1800 E. Paul Dirac Dr, Tallahassee, FL, 32310, USA ORCID: 0000-0002-3570-9787, Email: fmentink@magnet.fsu.edu

Authors

Satyaki Chatterjee: University of Iceland, Department of Chemistry, Science Institute, Dunhaga 3, 107 Reykjavik (Iceland). ORCID: 0000-0003-3543-7758

Faith J. Scott: National High Magnetic Field Laboratory, Florida State University, 1800 E. Paul Dirac Dr, Tallahassee, FL, 32310, USA. ORCID: 0000-0003-3903-8842

Snorri Th. Sigurdsson: University of Iceland, Department of Chemistry, Science Institute, Dunhaga 3, 107 Reykjavik (Iceland). ORCID: 0000-0003-2492-1456

Amrit Venkatesh: National High Magnetic Field Laboratory, Florida State University, 1800 E. Paul Dirac Dr, Tallahassee, FL, 32310. ORCID: 0000-0001-5319-9269

The authors declare no competing financial interests.

ACKNOWLEDGMENTS

The National High Magnetic Field Laboratory (NHMFL) is funded by the National Science Foundation Division of Materials Research (DMR-2128556) and the State of Florida. A portion of this work was supported by National Institutes of Health Grant RM1-GM148766. This project has received partial support from the European Union's Horizon 2020 research and innovation programme under Grant Agreement 101008500 (PANACEA). FJS acknowledges support by a Postdoctoral Scholar Award from the Provost's Office at Florida State University. This work was also supported by the Icelandic Research Fund (Grant 239662), the University of Iceland Research Fund (S.Th.S.), and a doctoral fellowship from the University of Iceland Research Fund (S.C.). FMV thanks Zhenfeng Peng and Kong Ooi Tan for fruitful discussions at the early stages of this work.

REFERENCES

(1) Reif, B.; Ashbrook, S. E.; Emsley, L.; Hong, M. Solid-State NMR Spectroscopy. *Nat. Rev. Methods Primer* **2021**, *1* (1), 1–23. https://doi.org/10.1038/s43586-020-00002-1.

(2) Lilly Thankamony, A. S.; Wittmann, J. J.; Kaushik, M.; Corzilius, B. Dynamic Nuclear Polarization for Sensitivity Enhancement in Modern Solid-State NMR. *Prog. Nucl. Magn. Reson. Spectrosc.* **2017**, *102–103*, 120–195. https://doi.org/10.1016/j.pnmrs.2017.06.002.

(3) Lee, D.; Hediger, S.; De Paëpe, G. Is Solid-State NMR Enhanced by Dynamic Nuclear Polarization? *Solid State Nucl. Magn. Reson.* **2015**, *66–67*, 6–20. https://doi.org/10.1016/j.ssnmr.2015.01.003.

(4) Rankin, A. G. M.; Trébosc, J.; Pourpoint, F.; Amoureux, J.-P.; Lafon, O. Recent Developments in MAS DNP-NMR of Materials. *Solid State Nucl. Magn. Reson.* **2019**, *101*, 116–143. https://doi.org/10.1016/j.ssnmr.2019.05.009.
(5) Chow, W. Y.; De Paëpe, G.; Hediger, S. Biomolecular and Biological Applications of Solid-State NMR with Dynamic Nuclear Polarization Enhancement. *Chem. Rev.* **2022**, *122* (10), 9795–9847. https://doi.org/10.1021/acs.chemrev.1c01043.
(6) Ghassemi, N.; Poulhazan, A.; Deligey, F.; Mentink-Vigier, F.; Marcotte, I.; Wang, T. Solid-State NMR Investigations of Extracellular Matrixes and Cell Walls of Algae, Bacteria, Fungi, and Plants. *Chem. Rev.* **2022**, *122* (10), 10036–10086. https://doi.org/10.1021/acs.chemrev.1c00669.
(7) Rossini, A. J.; Zagdoun, A.; Lelli, M.; Lesage, A.; Copéret, C.; Emsley, L. Dynamic Nuclear Polarization Surface Enhanced NMR Spectroscopy. *Acc. Chem. Res.* **2013**, *46* (9), 1942–1951. https://doi.org/10.1021/ar300322x.
(8) Ni, Q. Z.; Daviso, E.; Can, T. V.; Markhasin, E.; Jawla, S. K.; Swager, T. M.; Temkin, R. J.; Herzfeld, J.; Griffin, R. G. High Frequency Dynamic Nuclear Polarization. *Acc. Chem. Res.* **2013**, *46* (9), 1933–1941. https://doi.org/10.1021/ar300348n.
(9) Casano, G.; Karoui, H.; Ouari, O. Polarizing Agents: Evolution and Outlook in Free Radical Development for DNP. In *eMagRes*; 2018; Vol. 7, pp 195–208.
(10) Kundu, K.; Mentink-Vigier, F.; Feintuch, A.; Vega, S. DNP Mechanisms. In *eMagRes*; John Wiley & Sons, Ltd, 2019; pp 295–338. https://doi.org/10.1002/9780470034590.emrstm1550.
(11) Thurber, K. R.; Tycko, R. Theory for Cross Effect Dynamic Nuclear Polarization under Magic-Angle Spinning in Solid State Nuclear Magnetic Resonance: The Importance of Level Crossings. *J. Chem. Phys.* **2012**, *137* (8), 084508. https://doi.org/10.1063/1.4747449.
(12) Mentink-Vigier, F.; Akbey, Ü.; Hovav, Y.; Vega, S.; Oschkinat, H.; Feintuch, A. Fast Passage Dynamic Nuclear Polarization on Rotating Solids. *J. Magn. Reson.* **2012**, *224*, 13–21. https://doi.org/10.1016/j.jmr.2012.08.013.
(13) Thurber, K. R.; Tycko, R. Perturbation of Nuclear Spin Polarizations in Solid State NMR of Nitroxide-Doped Samples by Magic-Angle Spinning without Microwaves. *J. Chem. Phys.* **2014**, *140* (18), 184201. https://doi.org/10.1063/1.4874341.
(14) Mentink-Vigier, F.; Paul, S.; Lee, D.; Feintuch, A.; Hediger, S.; Vega, S.; De Paëpe, G. Nuclear Depolarization and Absolute Sensitivity in Magic-Angle Spinning Cross Effect Dynamic Nuclear Polarization. *Phys. Chem. Chem. Phys.* **2015**, *17* (34), 21824–21836. https://doi.org/10.1039/C5CP03457D.
(15) Mentink-Vigier, F.; Marin-Montesinos, I.; Jagtap, A. P.; Halbritter, T.; van Tol, J.; Hediger, S.; Lee, D.; Sigurdsson, S. Th.; De Paëpe, G. Computationally Assisted Design of Polarizing Agents for Dynamic Nuclear Polarization Enhanced NMR: The AsymPol Family. *J. Am. Chem. Soc.* **2018**, *140* (35), 11013–11019. https://doi.org/10.1021/jacs.8b04911.
(16) Scott, F. J.; Eddy, S.; Gullion, T.; Mentink-Vigier, F. Sorbitol-Based Glass Matrices Enable Dynamic Nuclear Polarization beyond 200 K. *J. Phys. Chem. Lett.* **2024**, 8743–8751. https://doi.org/10.1021/acs.jpclett.4c02054.
(17) Equbal, A.; Tagami, K.; Han, S. Balancing Dipolar and Exchange Coupling in Biradicals to Maximize Cross Effect Dynamic Nuclear Polarization. *Phys. Chem. Chem. Phys.* **2020**, *22* (24), 13569–13579. https://doi.org/10.1039/D0CP02051F.
(18) Equbal, A.; Leavesley, A.; Jain, S. K.; Han, S. Cross-Effect Dynamic Nuclear Polarization Explained: Polarization, Depolarization, and Oversaturation. *J. Phys. Chem. Lett.* **2019**, *10* (3), 548–558. https://doi.org/10.1021/acs.jpclett.8b02834.

(19) Tan, K. O.; Mardini, M.; Yang, C.; Ardenkjær-Larsen, J. H.; Griffin, R. G. Three-Spin Solid Effect and the Spin Diffusion Barrier in Amorphous Solids. *Sci. Adv.* **2019**, *5* (7), eaax2743. https://doi.org/10.1126/sciadv.aax2743.
(20) Stern, Q.; Cousin, S. F.; Mentink-Vigier, F.; Pinon, A. C.; Elliott, S. J.; Cala, O.; Jannin, S. Direct Observation of Hyperpolarization Breaking through the Spin Diffusion Barrier. *Sci. Adv.* **2021**, *7* (18), eabf5735. https://doi.org/10.1126/sciadv.abf5735.
(21) Wolfe, J. P. Direct Observation of a Nuclear Spin Diffusion Barrier. *Phys. Rev. Lett.* **1973**, *31* (15), 907–910. https://doi.org/10.1103/PhysRevLett.31.907.
(22) Wittmann, J. J.; Eckardt, M.; Harneit, W.; Corzilius, B. Electron-Driven Spin Diffusion Supports Crossing the Diffusion Barrier in MAS DNP. *Phys. Chem. Chem. Phys.* **2018**, *20* (16), 11418–11429. https://doi.org/10.1039/C8CP00265G.
(23) Karabanov, A.; Wiśniewski, D.; Lesanovsky, I.; Köckenberger, W. Dynamic Nuclear Polarization as Kinetically Constrained Diffusion. *Phys. Rev. Lett.* **2015**, *115* (2), 020404. https://doi.org/10.1103/PhysRevLett.115.020404.
(24) Mentink-Vigier, F.; Vega, S.; De Paëpe, G. Fast and Accurate MAS–DNP Simulations of Large Spin Ensembles. *Phys. Chem. Chem. Phys.* **2017**, *19* (5), 3506–3522. https://doi.org/10.1039/C6CP07881H.
(25) Mentink-Vigier, F.; Dubroca, T.; Van Tol, J.; Sigurdsson, S. Th. The Distance between G-Tensors of Nitroxide Biradicals Governs MAS-DNP Performance: The Case of the bTurea Family. *J. Magn. Reson.* **2021**, *329*, 107026. https://doi.org/10.1016/j.jmr.2021.107026.
(26) Perras, F. A.; Raju, M.; Carnahan, S. L.; Akbarian, D.; Van Duin, A. C. T.; Rossini, A. J.; Pruski, M. Full-Scale Ab Initio Simulation of Magic-Angle-Spinning Dynamic Nuclear Polarization. *J. Phys. Chem. Lett.* **2020**, *11* (14), 5655–5660. https://doi.org/10.1021/acs.jpclett.0c00955.
(27) Venkatesh, A.; Casano, G.; Rao, Y.; De Biasi, F.; Perras, F. A.; Kubicki, D. J.; Siri, D.; Abel, S.; Karoui, H.; Yulikov, M.; Ouari, O.; Emsley, L. Deuterated TEKPol Biradicals and the Spin-Diffusion Barrier in MAS DNP. *Angew. Chem. Int. Ed.* **2023**, *62* (31), e202304844. https://doi.org/10.1002/anie.202304844.
(28) Chatterjee, S.; Venkatesh, A.; Sigurdsson, S. Th.; Mentink-Vigier, F. Role of Protons in and around Strongly Coupled Nitroxide Biradicals for Cross-Effect Dynamic Nuclear Polarization. *J. Phys. Chem. Lett.* **2024**, *15* (8), 2160–2168. https://doi.org/10.1021/acs.jpclett.3c03472.
(29) Harrabi, R.; Halbritter, T.; Aussenac, F.; Dakhlaoui, O.; van Tol, J.; Damodaran, K. K.; Lee, D.; Paul, S.; Hediger, S.; Mentink-Vigier, F.; Sigurdsson, S. Th.; De Paëpe, G. Highly Efficient Polarizing Agents for MAS-DNP of Proton-Dense Molecular Solids. *Angew. Chem. Int. Ed.* **2022**, *61* (12), e202114103. https://doi.org/10.1002/anie.202114103.
(30) Perras, F. A.; Carnahan, S. L.; Lo, W.-S.; Ward, C. J.; Yu, J.; Huang, W.; Rossini, A. J. Hybrid Quantum-Classical Simulations of Magic Angle Spinning Dynamic Nuclear Polarization in Very Large Spin Systems. *J. Chem. Phys.* **2022**, *156* (12), 124112. https://doi.org/10.1063/5.0086530.
(31) Perras, F. A.; Reinig, R. R.; Slowing, I. I.; Sadow, A. D.; Pruski, M. Effects of Biradical Deuteration on the Performance of DNP: Towards Better Performing Polarizing Agents. *Phys. Chem. Chem. Phys.* **2016**, *18* (1), 65–69. https://doi.org/10.1039/C5CP06505D.
(32) Geiger, M.-A.; Orwick-Rydmark, M.; Märker, K.; Franks, W. T.; Akhmetzyanov, D.; Stöppler, D.; Zinke, M.; Specker, E.; Nazaré, M.; Diehl, A.; van Rossum, B.-J.; Aussenac, F.; Prisner, T.; Akbey, Ü.; Oschkinat, H. Temperature Dependence of Cross-Effect Dynamic

Nuclear Polarization in Rotating Solids: Advantages of Elevated Temperatures. *Phys. Chem. Chem. Phys.* **2016**, *18* (44), 30696–30704. https://doi.org/10.1039/C6CP06154K.
(33) Feher, G. Observation of Nuclear Magnetic Resonances via the Electron Spin Resonance Line. *Phys. Rev.* **1956**, *103* (3), 834–835. https://doi.org/10.1103/PhysRev.103.834.
(34) Zagdoun, A.; Casano, G.; Ouari, O.; Schwarzwälder, M.; Rossini, A. J.; Aussenac, F.; Yulikov, M.; Jeschke, G.; Copéret, C.; Lesage, A.; Tordo, P.; Emsley, L. Large Molecular Weight Nitroxide Biradicals Providing Efficient Dynamic Nuclear Polarization at Temperatures up to 200 K. *J. Am. Chem. Soc.* **2013**, *135* (34), 12790–12797. https://doi.org/10.1021/ja405813t.
(35) Sauvée, C.; Rosay, M.; Casano, G.; Aussenac, F.; Weber, R. T.; Ouari, O.; Tordo, P. Highly Efficient, Water-Soluble Polarizing Agents for Dynamic Nuclear Polarization at High Frequency. *Angew. Chem. Int. Ed.* **2013**, *52* (41), 10858–10861. https://doi.org/10.1002/anie.201304657.
(36) Harrabi, R.; Halbritter, T.; Alarab, S.; Chatterjee, S.; Wolska-Pietkiewicz, M.; Damodaran, K. K.; Van Tol, J.; Lee, D.; Paul, S.; Hediger, S.; Sigurdsson, S. Th.; Mentink-Vigier, F.; De Paëpe, G. AsymPol-TEKs as Efficient Polarizing Agents for MAS-DNP in Glass Matrices of Non-Aqueous Solvents. *Phys. Chem. Chem. Phys.* **2024**, *26* (6), 5669–5682. https://doi.org/10.1039/D3CP04271E.
(37) Ward, K. M.; Aletras, A. H.; Balaban, R. S. A New Class of Contrast Agents for MRI Based on Proton Chemical Exchange Dependent Saturation Transfer (CEST). *J. Magn. Reson.* **2000**, *143* (1), 79–87. https://doi.org/10.1006/jmre.1999.1956.
(38) Fawzi, N. L.; Ying, J.; Ghirlando, R.; Torchia, D. A.; Clore, G. M. Atomic-Resolution Dynamics on the Surface of Amyloid-β Protofibrils Probed by Solution NMR. *Nature* **2011**, *480* (7376), 268–272. https://doi.org/10.1038/nature10577.
(39) Long, D.; Bouvignies, G.; Kay, L. E. Measuring Hydrogen Exchange Rates in Invisible Protein Excited States. *Proc. Natl. Acad. Sci.* **2014**, *111* (24), 8820–8825. https://doi.org/10.1073/pnas.1405011111.
(40) Jaroszewicz, M. J.; Altenhof, A. R.; Schurko, R. W.; Frydman, L. Sensitivity Enhancement by Progressive Saturation of the Proton Reservoir: A Solid-State NMR Analogue of Chemical Exchange Saturation Transfer. *J. Am. Chem. Soc.* **2021**, *143* (47), 19778–19784. https://doi.org/10.1021/jacs.1c08277.
(41) Hyde, J. S.; Chien, J. C. W.; Freed, J. H. Electron–Electron Double Resonance of Free Radicals in Solution. *J. Chem. Phys.* **1968**, *48* (9), 4211–4226. https://doi.org/10.1063/1.1669760.
(42) Goldfarb, D. ELDOR-Detected NMR. In *eMagRes*; Harris, R. K., Wasylishen, R. L., Eds.; John Wiley & Sons, Ltd: Chichester, UK, 2017; pp 101–114. https://doi.org/10.1002/9780470034590.emrstm1516.
(43) Mentink-Vigier, F.; Akbey, Ü.; Oschkinat, H.; Vega, S.; Feintuch, A. Theoretical Aspects of Magic Angle Spinning - Dynamic Nuclear Polarization. *J. Magn. Reson.* **2015**, *258*, 102–120. https://doi.org/10.1016/j.jmr.2015.07.001.
(44) Pang, Z.; Sheberstov, K.; Rodin, B. A.; Lumsden, J.; Banerjee, U.; Abergel, D.; Bodenhausen, G.; Tan, K. O. Hypershifted Spin Spectroscopy with Dynamic Nuclear Polarization at 1.4 K. June 10, 2024. https://doi.org/10.26434/chemrxiv-2024-zr8zv.
(45) Stoll, S.; Schweiger, A. EasySpin, a Comprehensive Software Package for Spectral Simulation and Analysis in EPR. *J. Magn. Reson.* **2006**, *178* (1), 42–55. https://doi.org/10.1016/j.jmr.2005.08.013.

(46) Stoll, S. CW-EPR Spectral Simulations. In *Methods in Enzymology*; Elsevier, 2015; Vol. 563, pp 121–142. https://doi.org/10.1016/bs.mie.2015.06.003.
(47) Mentink-Vigier, F.; Barra, A.-L.; van Tol, J.; Hediger, S.; Lee, D.; De Paëpe, G. *De Novo* Prediction of Cross-Effect Efficiency for Magic Angle Spinning Dynamic Nuclear Polarization. *Phys. Chem. Chem. Phys.* **2019**, *21* (4), 2166–2176. https://doi.org/10.1039/C8CP06819D.
(48) Soetbeer, J.; Gast, P.; Walish, J. J.; Zhao, Y.; George, C.; Yang, C.; Swager, T. M.; Griffin, R. G.; Mathies, G. Conformation of Bis-Nitroxide Polarizing Agents by Multi-Frequency EPR Spectroscopy. *Phys. Chem. Chem. Phys.* **2018**, *20* (39), 25506–25517. https://doi.org/10.1039/C8CP05236K.
(49) Can, T. V.; Caporini, M. A.; Mentink-Vigier, F.; Corzilius, B.; Walish, J. J.; Rosay, M.; Maas, W. E.; Baldus, M.; Vega, S.; Swager, T. M.; Griffin, R. G. Overhauser Effects in Insulating Solids. *J. Chem. Phys.* **2014**, *141* (6), 064202. https://doi.org/10.1063/1.4891866.
(50) Ji, X.; Can, T. V.; Mentink-Vigier, F.; Bornet, A.; Milani, J.; Vuichoud, B.; Caporini, M. A.; Griffin, R. G.; Jannin, S.; Goldman, M.; Bodenhausen, G. Overhauser Effects in Non-Conducting Solids at 1.2 K. *J. Magn. Reson.* **2018**, *286*, 138–142. https://doi.org/10.1016/j.jmr.2017.11.017.
(51) Jardón-Álvarez, D.; Leskes, M. Metal Ions Based Dynamic Nuclear Polarization: MI-DNP. *Prog. Nucl. Magn. Reson. Spectrosc.* **2023**, *138–139*, 70–104. https://doi.org/10.1016/j.pnmrs.2023.08.002.